

THE EFFECT OF TYPE OF ACID SITES IN MOLECULAR SIEVES ON ACTIVITY AND SELECTIVITY IN ACYLATION REACTIONS

Martina BEJBLOVÁ^{1,*}, Josef VLK², Dana PROCHÁZKOVÁ³, Helena ŠIKLOVÁ⁴ and Jiří ČEJKA⁵

J. Heyrovský Institute of Physical Chemistry, Academy of Sciences of the Czech Republic, v.v.i., Dolejškova 3, CZ-182 23, Prague 8, Czech Republic; e-mail: ¹ martina.bejblova@jh-inst.cas.cz, ² josef.vlk@vscht.cz, ³ prochazkova@jh-inst.cas.cz, ⁴ siklova@jh-inst.cas.cz, ⁵ cejka@jh-inst.cas.cz

Received February 1, 2007

Accepted April 2, 2007

Dedicated to Dr Karel Mach on the occasion of his 70th birthday.

The role of the type of acid site (Broensted vs. Lewis) on the activity and selectivity of molecular sieve catalysts was investigated in ferrocene and toluene acylation. H-, Zn-, Fe-, Al- and La-forms of zeolite Beta, USY and mesoporous molecular sieves (Al)MCM-41, (Al)SBA-15 were tested. It was observed that addition of metal cations acting as Lewis acid sites can increase the acidity of various molecular sieve catalysts. No general relationship between the type of cation and conversion of individual substrate was found. While the highest activity in ferrocene acylation was observed after addition of Zn, in the case of toluene acylation Al-forms of catalysts were the most active. The results indicate that the acid strength of cationic Lewis sites controls their activity in acylation reactions.

Keywords: Molecular sieves; Zeolites; Acylations; Ferrocene; Toluene.

Zeolites are widely used in organic synthesis¹, petrochemical processes² and in the synthesis of fine chemicals³. The key properties in the use of zeolites as acid catalysts are tuned acidity, controlled site density, high thermal and hydrothermal stability, and shape selectivity towards reactants, products, and transition states^{4,5}. Friedel–Crafts acylations are reactions, in which zeolites are the most promising group of catalysts. They could replace traditional catalysts (AlCl₃, FeCl₃, BF₃, TiCl₄, ZnCl₂ or phosphoric acid), the application of which brings ecological and technical problems. In addition, Lewis acids form stable complexes with products, which have to be decomposed with water.

Successful application of zeolite catalysts in the Friedel–Crafts acylation of aromatics has been described in literature. Attention has been especially paid to acylation reactions producing aromatic ketones, which can be used in

fine chemical industries. Naphthalene⁶, toluene^{7,8}, 2-methoxynaphthalene^{9,10}, phenol^{11,12}, anisole^{13,14}, veratrole^{15,16} and isobutylbenzene¹⁷ belong to the most frequently investigated substrates. Zeolite Beta was distinguished as a highly active and selective catalyst in acylation of bulkier substrates. Various acyl halides, acid anhydrides or carboxylic acids were used as acylating agents in these reactions.

The conventional homogeneous catalysts in acylation reactions are of both Brønsted and Lewis acid types. With regard to that, zeolite acidity can be varied in a significant range as far as the type and concentration of acid sites are concerned. The objective of this contribution is to evaluate the effect of the acid site type on the activity of zeolites USY and Beta and mesoporous molecular sieves (Al)MCM-41 and (Al)SBA-15 in acylation of ferrocene and toluene.

Acylation of ferrocene leads to the formation of acylferrocenes, which are used as intermediates in the production of functional materials like functional polymers, chiral catalysts, combustion catalysts for propellants, pharmaceuticals, etc.¹⁸.

Acylation of toluene with derivatives of isobutyric acid is the model reaction of the first reaction step in the synthesis of Ibuprofen. In our previous paper, we have shown that toluene (as a less toxic substrate compared with benzene) can be easily acylated using acid forms of large-pore zeolites, such as ultrastable zeolite Y and Beta⁸.

EXPERIMENTAL

Catalysts

Zeolites Beta and USY, and mesoporous molecular sieves (Al)MCM-41 and (Al)SBA-15, and their ion-exchanged forms (Zn^{2+} , Fe^{3+} , La^{3+} and Al^{3+}) were tested in acylation reactions of ferrocene and toluene. The list of catalysts used with their structure characterization, pore dimensions and Si/Al ratios is given in Table I.

All the catalysts were used in acylation reactions in protonated (H^+) and ion-exchanged forms (Zn^{2+} , Fe^{3+} , La^{3+} and Al^{3+}).

Ion-exchanged forms (Zn^{2+} , Fe^{3+} , La^{3+} and Al^{3+}) of molecular sieves were prepared by the following procedure. Zeolites were converted to sodium forms by four times repeated ion exchange with 0.5 M sodium nitrate at room temperature for 4 h. Then the Na-forms were transformed to corresponding cation forms via four times repeated ion exchange with 0.25 M nitrate of the respective element at room temperature for 4 h. Finally, molecular sieves were recovered by filtration, washed out with distilled water, dried and calcined at 550 °C for 6 h of a heating rate of 1 °C/min.

Synthesis of (Al)MCM-41 and (Al)SBA-15

For the synthesis of (Al)MCM-41, sodium silicate, aluminium isopropoxide and trimethyltetradecylammonium bromide as template were used. In a typical synthesis, 9.81 g of trimethyltetradecylammonium bromide was dissolved in 500 ml of water in an autoclavable polypropylene bottle, then 1.12 g of aluminum isopropoxide was added and this mixture was stirred for ca. 1 h. Later on, 450 ml of water was added, followed by 10 g of sodium silicate and it was stirred for 30 min. Finally, 15 ml of ethyl acetate was added, the mixture was aged at room temperature for 5 h and then at 90 °C for 2 days.

Mesoporous molecular sieve SBA-15 was prepared according to the following procedure¹⁹: 20 g of triblock copolymer poly(ethylene oxide)–poly(propylene oxide)–poly(ethylene oxide), EO₂₀PO₇₀EO₂₀ (template) were dissolved in 645 ml of water and 106 ml of 35% HCl and stirred at 35 °C. Then 45.5 ml of tetraethoxysilane were added to the clear solution and the mixture was stirred until became homogeneous. The mixture was allowed to stand at 35 °C for 24 h and subsequently at 95 °C for 48 h. The resulting solid phase was recovered by filtration, washed with distilled water and ethanol, and dried at room temperature. Calcination was carried out at 540 °C for 8 h with temperature ramp of 1 °C/min.

Aluminum was added to the SBA-15 samples by post-synthesis alumination²⁰. The reaction mixture of 5 g of SBA-15 and 1 g of aluminum chlorohydrate in 125 ml of distilled water was heated at 80 °C for 2 h. The solid was recovered by filtration, washed with water and dried at ambient temperature. Calcination was carried out at 550 °C for 4 h with temperature ramp of 1 °C/min.

Characterization of Catalysts

The crystallinity of zeolites was determined by X-ray powder diffraction with a Bruker D8 X-ray powder diffractometer equipped with a graphite monochromator and position-sensitive detector using CuK α radiation in the Bragg–Brentano geometry.

The concentration and the type of acid sites were determined by adsorption of acetonitrile-*d*₃ or pyridine as probe molecules followed by FTIR spectroscopy (Nicolet Protégé 460) using the self-supported wafer technique. Prior to adsorption of probe molecules, self-supporting wafers of catalysts were activated in situ by overnight evacuation at

TABLE I
Structural and chemical characteristics of used catalysts

Zeolite	Origin	Channel structure	Channel diameter, nm	Si/Al ratio
Beta	Zeolyst	3D	0.64 × 0.70 and 0.56 × 0.56	12.5
USY	Zeolyst	3D	0.74	15
MCM-41	synthesized	1D	~3.4	8.5
SBA-15	synthesized	1D	~6.5	14

450 °C. Adsorption of acetonitrile- d_3 proceeded at room temperature for 30 min at a partial pressure of 950 Pa and was followed by 20-min evacuation. To obtain quantitative analysis, the molar absorption coefficients²¹ for acetonitrile- d_3 adsorbed on Brønsted acid sites ($\nu(\text{C}\equiv\text{N})\text{-B}$ at 2297 cm^{-1} , $\epsilon(\text{B}) = 2.05 \pm 0.1\text{ cm } \mu\text{mol}^{-1}$) and strong and weak Lewis acid sites ($\nu(\text{C}\equiv\text{N})\text{-L}_1$ at 2325 cm^{-1} and $\nu(\text{CN})\text{-L}_2$ at 2310 cm^{-1} , respectively, $\epsilon(\text{L}) = 3.6 \pm 0.2\text{ cm } \mu\text{mol}^{-1}$) were used. Integral intensities of individual bands were used and spectra were normalized to the wafer thickness 10 mg cm^{-2} .

Adsorption of pyridine proceeded at 150 °C for 20 min at partial pressure 900 Pa followed by 15-min evacuation. The concentrations of Brønsted and Lewis acid sites were calculated from integral intensities of individual bands characteristic of pyridine on Brønsted acid sites at 1545 cm^{-1} and band of pyridine on Lewis acid site at 1455 cm^{-1} and molar absorption coefficients²² of $\epsilon(\text{B}) = 1.67 \pm 0.1\text{ cm } \mu\text{mol}^{-1}$ and $\epsilon(\text{L}) = 2.22 \pm 0.1\text{ cm } \mu\text{mol}^{-1}$, respectively (Table II). The spectra were recorded with a resolution of 4 cm^{-1} by collection 64 scans for single spectrum.

Chemical analysis was carried out by X-ray fluorescence analysis using a spectrometer Philips PW 1404 provided with an analytical program UniQuant.

Catalytic Experiments

Acylation reactions were investigated in a Heidolph Synthesis 1 (system of 16 parallel reactors) in a liquid phase under atmospheric pressure. Prior to catalytic experiments, each zeolite was activated at 450 °C for 90 min and then cooled in a desiccator. Reaction products

TABLE II
Concentrations of Brønsted (BC) and Lewis (LC) acid sites obtain by FTIR spectroscopy

Zeolite	FTIR, CD_3CN		Zeolite	FTIR, pyridine	
	c_{LC} mmol/g	c_{BC} mmol/g		c_{LC} mmol/g	c_{BC} mmol/g
H-Beta	0.30	0.26	H-(Al)MCM-41	0.21	0.04
Zn-Beta	0.47	0.07	Zn-(Al)MCM-41	0.40	0.04
Fe-Beta	0.15	0.07	Fe-(Al)MCM-41	0.10	0.01
La-Beta	0.24	0.06	La-(Al)MCM-41	0.16	0.04
Al-Beta	0.35	0.05	Al-(Al)MCM-41	0.27	0.04
H-USY	0.16	0.12	H-(Al)SBA-15	0.15	0.01
Zn-USY	0.30	0.12	Zn-(Al)SBA-15	0.28	0.02
Fe-USY	0.12	0.05	Fe-(Al)SBA-15	0.16	0.02
La-USY	0.15	0.02	La-(Al)SBA-15	0.11	0.01
AlH-USY	0.36	0.06	Al-(Al)SBA-15	0.17	0.03

were analyzed on a gas chromatograph (HP 6850 with FID detector) equipped with a high-resolution capillary column DB-5 (length 10 m, diameter 0.10 mm, phase thickness 0.10 μm).

Acylation of ferrocene. In a typical experiment, 0.6 g of ferrocene (Fluka), 8 ml of decahydronaphthalene (Fluka; solvent), dodecane (Aldrich; internal standard) and 0.6 g of an activated catalyst were heated to the preset reaction temperature. Then 1.9 ml of acetic anhydride (Fluka) were added to the reaction mixture and the reaction started. The reaction temperature was 140 °C. Selectivity (S) to acetylferrocene was calculated:

$$S = \frac{n}{\sum n_i}, \quad (1)$$

where n means the molar amount of acetylferrocene and n_i the molar amount of the reaction product i .

Acylation of toluene. In a typical experiment, 8.0 ml of toluene (Lachema, Czech Republic), dodecane (Aldrich; internal standard) and 0.7 g of an activated catalyst were heated to the preset reaction temperature. Then 1.9 ml of isobutyryl chloride (Fluka) were added to the mixture and the reaction was started. The reaction temperature was 110 °C. Selectivity (S) to isopropyl p -tolyl ketone was calculated from Eq. (1), where n was the molar amount of isopropyl p -tolyl ketone and n_i the molar amount of the reaction product i .

RESULTS AND DISCUSSION

Characterization of Acidity

FTIR spectra of zeolites Beta and USY in the region of OH vibrations consist of bands at 3745 cm^{-1} corresponding to the terminal silanol groups and bands characteristic of bridging OH groups in zeolite Beta at 3610 cm^{-1} and in zeolite USY at 3630 and 3565 cm^{-1} (Figs 1A and 2A). No band was observed in the region of Al-OH groups (ca. 3650–3660 cm^{-1}). A low-intensity band at 3782 cm^{-1} , frequently assigned to OH groups on extraframework aluminum oxide, was observed only in the spectra of Al^{3+} -forms of zeolite Beta and USY.

The adsorption of acetonitrile- d_3 resulted in complete disappearance of bands of bridging OH groups and formation of new absorption bands at 2297 and 2326 cm^{-1} characteristic of the adsorption of acetonitrile- d_3 on Si-OH-Al groups and on Al-Lewis sites, respectively (Figs 1B and 2B). In the case of ion-exchanged forms of zeolites Beta and USY it can be observed that some amount of bridging groups remained after the ion exchange, as expected when using divalent or even trivalent cations. This is also in agreement with chemical analysis data (Table III) showing the M/Al ratios lower than 1.

The individual maxima of absorption bands corresponding to the adsorption of acetonitrile- d_3 on Lewis sites show a relationship between the wavenumber and acid strength of the respective Lewis acid site. The order of acid strength is Al (2325 cm^{-1}) > Zn (2310 cm^{-1}) > Fe (2300 cm^{-1}) > La (2275 cm^{-1}). It should be noted that overlapping of absorption bands of acetonitrile- d_3 interacting with Si-OH-Fe groups as well as with Fe-Lewis

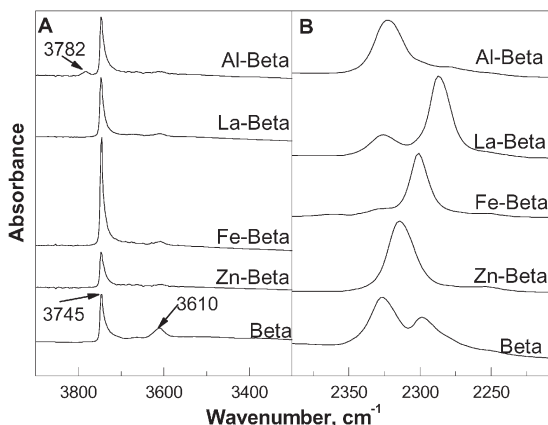


FIG. 1

IR spectra in the OH vibration region of zeolite Beta and its ion-exchanged forms before acetonitrile- d_3 adsorption (A) and spectra of acetonitrile- d_3 region after adsorption (B)

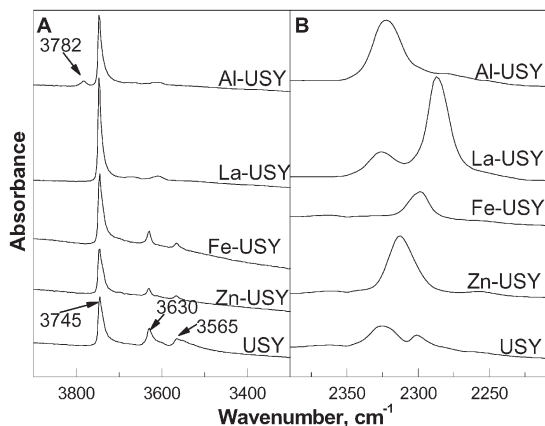


FIG. 2

IR spectra in the OH vibration region of zeolite USY and its ion-exchanged forms before acetonitrile- d_3 adsorption (A) and spectra of acetonitrile- d_3 region after adsorption (B)

acid sites was observed for both Fe-forms of zeolites Beta as well as USY (the absorption band with maximum around 2300 cm^{-1}).

The concentrations of Lewis and Brønsted acid sites in the samples were calculated using the molar absorption coefficients²¹ 3.6 ± 0.2 and $2.05 \pm 0.1\text{ cm}^2\text{ mol}^{-1}$, respectively. The results are given in Table II. The highest concentration of Lewis acid sites was found for the ion-exchanged Zn^{2+} -form of zeolite Beta. The concentrations decreased in the order $\text{Al} > \text{H} > \text{La} > \text{Fe}$. In zeolite USY the order of the Lewis acid site concentrations was $\text{Al} > \text{Zn} > \text{H} > \text{La} > \text{Fe}$.

FTIR spectra of (Al)MCM-41 and (Al)SBA-15 contain in the OH regions only a band at 3745 cm^{-1} corresponding to the terminal silanol groups (Figs 3A and 4A). The absorption band at 3660 cm^{-1} of OH groups on alumina was not observed and no absorption band in the region $3600\text{--}3610\text{ cm}^{-1}$ was found, which means that no bridging Si-OH-Al groups are present in the molecular sieves.

TABLE III
The degree of ion exchange of catalysts used

Zeolite	M^{n+}	M^{n+} , wt%	M^{n+}/Al ratio
BETA	Zn^{2+}	3.0	0.40
	Fe^{3+}	1.8	0.87
	La^{3+}	2.7	0.20
	Al^{3+}	1.2 ^a	0.29
USY	Zn^{2+}	2.6	0.49
	Fe^{3+}	2.1	0.56
	La^{3+}	3.2	0.33
	Al^{3+}	1.8 ^a	0.45
(Al)MCM-41	Zn^{2+}	3.5	0.34
	Fe^{3+}	2.7	2.7
	Al^{3+}	1.9 ^a	0.32
(Al)SBA-15	Zn^{2+}	1.7	0.29
	Fe^{3+}	0.89	1.15
	Al^{3+}	0.7 ^a	0.22

^a Al^{3+} added by ion exchange.

To obtain a quantitative analysis of the concentration of Brønsted and Lewis acid sites, pyridine adsorption was used for both molecular sieves (Al)MCM-41 and (Al)SBA-15 (Figs 3B and 4B). Pyridine adsorption resulted in the formation of a new band at 1455 cm^{-1} , which corresponds to the interaction between pyridine and Lewis acid²³. The intensity of this band decreased in the order: Zn > Al > H > La > Fe for (Al)MCM-41 and Zn > Al >

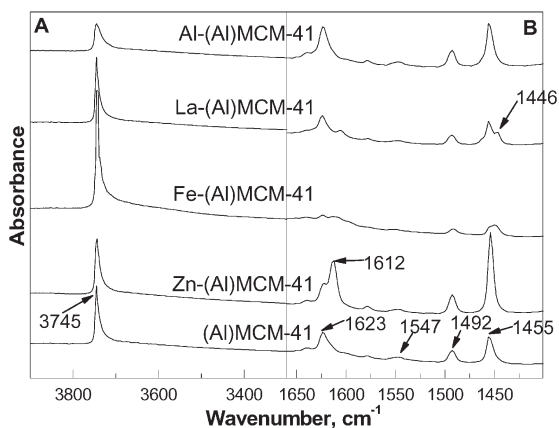


FIG. 3

IR spectra in the OH vibration region of (Al)MCM-41 and its ion-exchanged forms before pyridine adsorption (A) and spectra of pyridine region after adsorption (B)

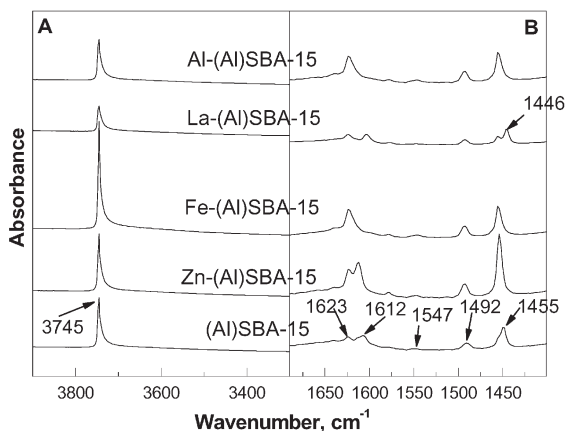


FIG. 4

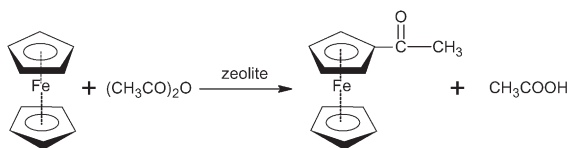
IR spectra in the OH vibration region of (Al)SBA-15 and its ion-exchanged forms before pyridine adsorption (A) and spectra of pyridine region after adsorption (B)

H > Fe > La for (Al)SBA-15. In La-forms of both mesoporous molecular sieves, formation of a new band at 1446 cm^{-1} was observed. This band indicates the presence of another type of Lewis acid site. The signal at 1623 cm^{-1} is assigned also to pyridine ions on Lewis acid sites. Only a negligible band at 1547 cm^{-1} corresponding to pyridinium ion (PyH^+) was found in the samples. This indicates that practically no acid OH groups are present in the mesoporous materials under investigation. The absorption band at 1492 cm^{-1} is assigned to pyridine adsorbed on both Brønsted and Lewis acid sites. In Zn- and La-forms of mesoporous molecular sieves, a new signal appears at ca. 1612 cm^{-1} . The resulting concentrations of Lewis and Brønsted acid sites calculated using molar absorption coefficients 2.22 ± 0.1 and $1.67 \pm 0.1\text{ cm}^2\text{ mol}^{-1}$, respectively, are given in Table II. The spectra in Figs 3B and 4B clearly show that there are no substantial differences between the wavenumbers of bands of pyridine coordinated to different Lewis acid sites as it was in the case of acetonitrile- d_3 adsorption in cation-exchanged zeolites.

The concentration of cations in catalysts was determined by X-ray fluorescence analysis. The degree of ion exchange determined from the M^{n+}/Al ratio is provided in Table III. These data are in agreement with FTIR spectra of acetonitrile- d_3 adsorption showing incomplete ion exchange of acid OH groups.

Acylation of Ferrocene

Friedel–Crafts acylation of ferrocene with acetic anhydride leads to the formation of acetylferrocenes. This reaction catalyzed by zeolites is highly selective to monoacetylferrocene (Scheme 1).



SCHEME 1

Zeolites Beta, USY and mesoporous molecular sieves (Al)MCM-41 and (Al)SBA-15 were tested as catalysts in acylation of ferrocene with acetic anhydride. As both Lewis and Brønsted acid sites exhibit catalytic activity in ferrocene acylation, the ion-exchanged forms with Zn^{2+} , Fe^{3+} , La^{3+} , Al^{3+} of these molecular sieves were prepared and we investigated the effect of the type of Lewis acid on the ferrocene conversion.

Figures 5–8 clearly depict the effect of the presence of added Lewis acid sites on the ferrocene conversion. In the case of zeolite Beta (Fig. 5), the highest conversion of ferrocene was found for Al-Beta and Zn-Beta zeolites.

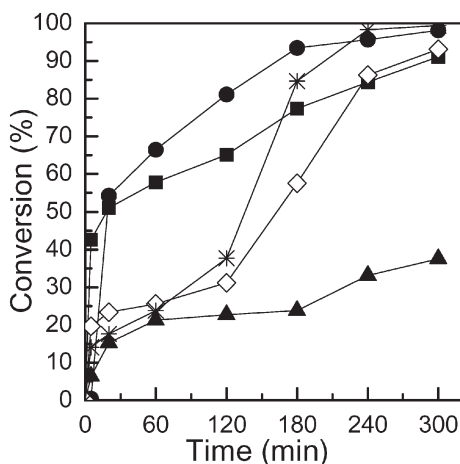


FIG. 5

The effect of active site types on the conversion of ferrocene in ferrocene acylation with acetic anhydride over ion-exchanged forms of zeolite Beta: H-Beta (■), Zn-Beta (●), Fe-Beta (▲), La-Beta (◇) and Al-Beta (*). Ferrocene/acetic anhydride ratio 1:6

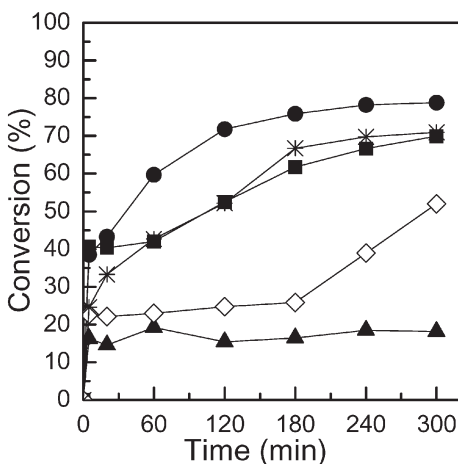


FIG. 6

The effect of active site types on the conversion of ferrocene in ferrocene acylation with acetic anhydride over ion-exchanged forms of zeolite USY: H-USY (■), Zn-USY (●), Fe-USY (▲), La-USY (◇) and Al-USY (*). Ferrocene/acetic anhydride ratio 1:6

Conversion of ferrocene over Zn-Beta was markedly lower up to 150 min of the time-on-stream (TOS) compared with Al-Beta. After 240 min of the reaction, the conversions over both catalysts were nearly the same reaching almost 100%. The ferrocene conversions over La-Beta and H-Beta after 300 min of the TOS were ca. 90%. However, the initial activity of these zeolites differed significantly. After 60 min of the TOS, the ferrocene conversion over H-Beta was 58% while the conversion over La-Beta was only 22%. The lowest ferrocene conversion was achieved with Fe-Beta (38% after 300-min reaction). The order of the increasing ferrocene conversion corresponds to the increasing concentration of Lewis acid sites determined by adsorption of acetonitrile- d_3 and FTIR spectroscopy. The highest concentration of Lewis acid sites was found for Zn-Beta and Al-Beta zeolites.

As to zeolite USY (Fig. 6), the highest ferrocene conversion was achieved again over Zn-Beta (ca. 80% after 300 min of TOS). Some decrease in the ferrocene conversion was observed with Al- and H-forms. The conversion of ferrocene over these two zeolites was ca. 10% lower in comparison with Zn-USY. The lowest ferrocene conversion was again found for Fe-USY. The results are in good agreement with the concentration of Lewis acid sites in USY zeolites. Al- and Zn-forms exhibited the highest concentration of Lewis acid sites while Fe-USY exhibited a 4.5 times lower concentration of Lewis acid sites.

With mesoporous molecular sieve (Al)MCM-41 (Fig. 7), the highest conversion of ferrocene was reached with H-form (about 90%). Some decrease in the conversion was observed over Zn-(Al)MCM-41 (71%) and the lowest conversion was again obtained over Fe-(Al)MCM-41.

Very similar results were obtained with (Al)SBA-15 (Fig. 8); however, the activity of Zn- and H-(Al)SBA-15 were comparable. Al-forms of mesoporous molecular sieves were not so active in ferrocene acylation as the forms prepared from zeolites Beta and USY.

It is well known that heat treatment of zeolites above 600 °C leads to dehydroxylation of Brønsted acid sites. Molecules of water are split off with concomitant formation of Lewis acid sites. We tried to study the effect of acid sites in ferrocene acylation in this way. Before acylation reaction, H-Beta was activated at 800 °C for 90 min and, after cooling, this zeolite was used in ferrocene acylation. We compared the ferrocene conversions obtained with zeolite activated at 450 and at 800 °C, in which we assumed increasing concentration of Lewis acid sites at the expense of Brønsted acid sites. Figure 9 clearly depicts the effect of activation temperature on the ferrocene conversion. The conversion of ferrocene was about 8% higher after 300 min of TOS with zeolite Beta activated at 800 °C.

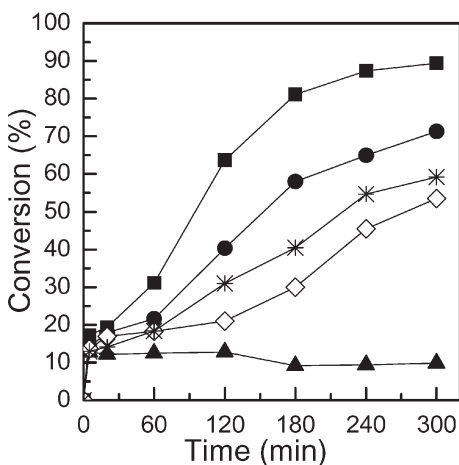


FIG. 7

The effect of active site types on the conversion of ferrocene in ferrocene acylation with acetic anhydride over ion-exchanged forms of zeolite (Al)MCM-41: H-(Al)MCM-41 (■), Zn-(Al)MCM-41 (●), Fe-(Al)MCM-41 (▲), La-(Al)MCM-41 (◇) and Al-(Al)MCM-41 (*). Ferrocene/acetic anhydride ratio 1:6

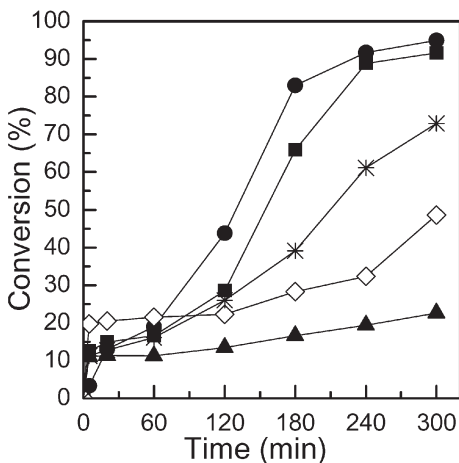


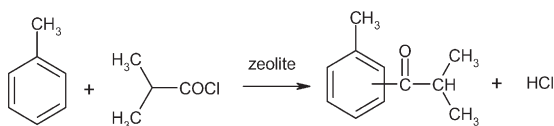
FIG. 8

The effect of active site types on the conversion of ferrocene in ferrocene acylation with acetic anhydride over ion-exchanged forms of zeolite (Al)SBA-15: H-(Al)SBA-15 (■), Zn-(Al)SBA-15 (●), Fe-(Al)SBA-15 (▲), La-(Al)SBA-15 (◇) and Al-(Al)SBA-15 (*). Ferrocene/acetic anhydride ratio 1:6

All these data clearly show that the presence of proper Lewis acid sites is crucial for achievement of high activity in ferrocene acylation with acetic anhydride. Ferrocene conversion increases with increasing concentration of Lewis acid sites and probably also the strength of these sites influences the resulting ferrocene conversion.

Acylation of Toluene

Toluene acylation with isobutyryl chloride is a model reaction for the synthesis of isopropyl tolyl ketones (Scheme 2). This reaction produces all three isomers of isopropyl tolyl ketone with preference for para isomer,



SCHEME 2

which is the main product of toluene acylation over zeolites due to shape-selectivity. For H-forms of zeolites, the selectivity to particular isomers depends on the level of isobutyryl chloride conversion, on the concentration of acid sites, and on the structure of the zeolite used⁸.

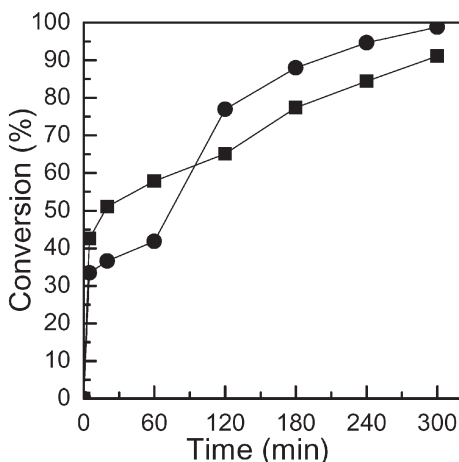


FIG. 9

The effect of activation temperature on the conversion of ferrocene in ferrocene acylation with acetic anhydride over zeolite BETA: 450 °C (■), 800 °C (●). Ferrocene/acetic anhydride ratio 1:6

Zeolites Beta and USY and mesoporous molecular sieves (Al)MCM-41 and (Al)SBA-15 and their ion-exchanged forms (Zn^{2+} , Fe^{3+} , La^{3+} and Al^{3+}) were investigated in acylation of toluene. The effect of the presence of added Lewis acid sites on the isobutyryl chloride conversion is clearly seen in Figs 10–13.

Al-, Zn- and La-forms of zeolite Beta showed very similar conversions of isobutyryl chloride (Fig. 10). The conversion of isobutyryl chloride obtained over these zeolites was in the range 80–85% after 240 min of TOS. The lowest isobutyryl chloride conversion reached ca. 57% with the ion-exchanged Fe^{3+} -form. When we compared these results with concentration of Lewis acid sites of zeolite Beta and its ion-exchanged forms obtained by adsorption of acetonitrile- d_3 and FTIR spectroscopy, we can see that with increasing concentration of Lewis acid sites the achieved conversion of the acylating agent increases. This is in a good agreement with the results obtained in ferrocene acylation.

In the case of zeolite USY, again very similar conversions of isobutyryl chloride were obtained for all the tested forms of this zeolite (Fig. 11). The conversions ranged from 43 to 55% after 240 min of TOS. The highest conversion was found for the Al-form possessing the highest concentration of Lewis acid sites and the lowest concentration of Brønsted acid sites.

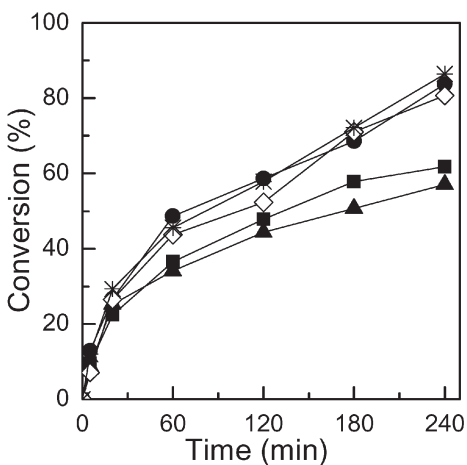


FIG. 10

The effect of active site types on the conversion of isobutyryl chloride in toluene acylation over ion-exchanged forms of zeolite Beta: H-Beta (■), Zn-Beta (●), Fe-Beta (▲), La-Beta (◇) and Al-Beta (*)

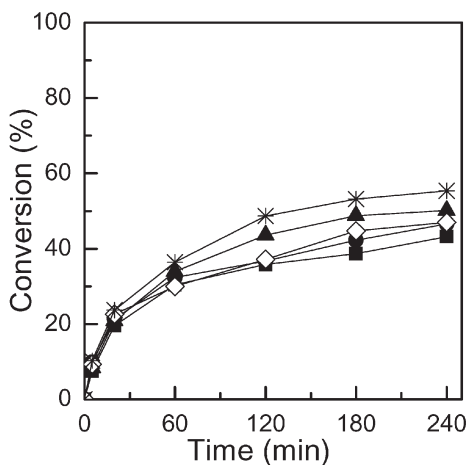


FIG. 11

The effect of active site types on the conversion of isobutyryl chloride in toluene acylation over ion-exchanged forms of zeolite USY: H-USY (■), Zn-USY (●), Fe-USY (▲), La-USY (◇) and Al-USY (*)

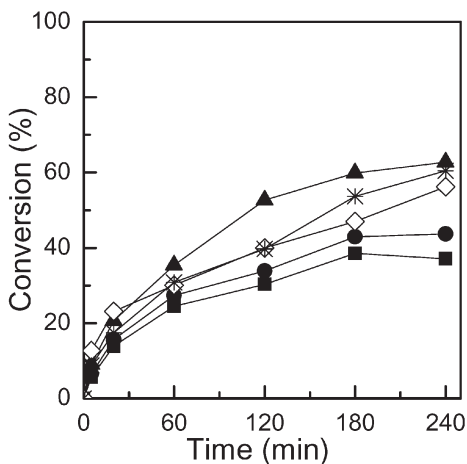


FIG. 12

The effect of active site types on the conversion of isobutyryl chloride in toluene acylation over ion-exchanged forms of zeolite (Al)MCM-41: H-(Al)MCM-41 (■), Zn-(Al)MCM-41 (●), Fe-(Al)MCM-41 (▲), La-(Al)MCM-41 (◇) and Al-(Al)MCM-41 (*)

Ion-exchanged Al^{3+} -forms of mesoporous molecular sieves (Al)MCM-41 and (Al)SBA-15 (Figs 12 and 13) were highly active catalysts in toluene acylation. Surprisingly, the conversion of isobutyryl chloride over Fe-(Al)MCM-41 was about 62% while in ferrocene acylation Fe-(Al)MCM-41 showed a very low activity. This indicates that Fe-Lewis acid sites easily activate toluene in contrast to ferrocene. H-forms of both mesoporous molecular sieves were not so active in toluene acylation as in the acylation of ferrocene. The conversion of isobutyryl chloride in toluene acylation over H-(Al)MCM-41 was only 37% and in the case of H-(Al)SBA-15 43%.

Selectivities to isopropyl *p*-tolyl ketone at the conversion 20% over zeolite Beta, USY, and their ion-exchanged forms with the exception of Fe-forms were higher than 80% (Fig. 14). The selectivity to para isomer with H-, Zn-, Al- and La-Beta ranged from 92 to 95%, over Fe-Beta it was ca. 78%. In the case of zeolite USY, the highest selectivity to isopropyl *p*-tolyl ketone was achieved with the La- and H-forms (96 and 98%, respectively). Again, the lowest selectivity (66%) to isopropyl *p*-tolyl ketone was reached with Fe-USY. In analogy with another para-selective reaction (toluene alkylation with ethene²⁴), it can be speculated that Fe cations are also highly active in subsequent isomerization, which substantially decreases the selectivity to para isomer.

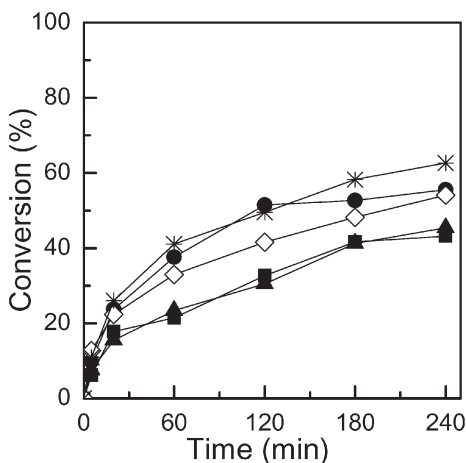


FIG. 13

The effect of active site types on the conversion of isobutyryl chloride in toluene acylation over ion-exchanged forms of zeolite (Al)SBA-15: H-(Al)SBA-15 (■), Zn-(Al)SBA-15 (●), Fe-(Al)SBA-15 (▲), La-(Al)SBA-15 (◇) and Al-(Al)SBA-15 (*)

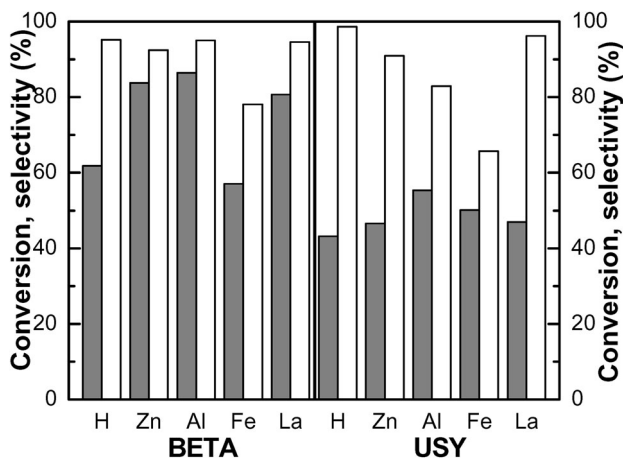


FIG. 14

The effect of active site types on the conversion of isobutyryl chloride and selectivity to isopropyl *p*-tolyl ketone in toluene acylation over ion-exchanged forms of zeolites Beta and USY: ■ conversion (at 240 min), □ selectivity (at isobutyryl chloride conversion 20%)

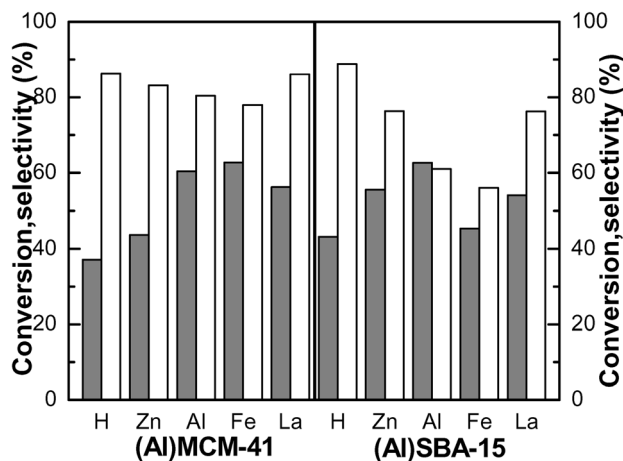


FIG. 15

The effect of active site types on the conversion of isobutyryl chloride and selectivity to isopropyl *p*-tolyl ketone in toluene acylation over ion-exchanged forms of (Al)MCM-41 and (Al)SBA-15: ■ conversion (at 240 min), □ selectivity (at isobutyryl chloride conversion 20%)

The selectivities to isopropyl *p*-tolyl ketone at the conversion of isobutyryl chloride of 20% over mesoporous molecular sieves (Al)MCM-41 and (Al)SBA-15 and their ion-exchanged forms were a little lower compared with the zeolites used (Fig. 15). This is due to larger channel diameters of these materials, which enable the formation of the bulkier *ortho*-isomer and also consecutive acylation of toluene to diisobutyryltoluenes. The selectivity to *para*-isomers over (Al)MCM-41 ranged from 78 to 86%. The lowest selectivities compared with other molecular sieves, were obtained over ion-exchanged forms of (Al)SBA-15.

CONCLUSIONS

The role of the acid site type (Broensted vs. Lewis) in the activity and selectivity of different molecular sieve catalysts was investigated in acylation of ferrocene with acetic anhydride and in acylation of toluene with isobutyryl chloride. H-, Zn-, Fe-, Al- and La-forms of zeolite Beta, USY and mesoporous molecular sieves (Al)MCM-41 and (Al)SBA-15 were investigated.

The concentration of Lewis and Broensted acid sites was determined by adsorption of acetonitrile- d_3 or pyridine as probe molecules followed by FTIR spectroscopy. The highest concentrations of Lewis acid sites were found for Zn- and Al-forms of the molecular sieves used. On the other hand, the lowest concentration of Lewis acid sites was found for the Fe-forms.

No general relationship between the type of cation and substrate was found. In acylation of ferrocene over zeolites Beta and USY, the highest conversions of ferrocene were achieved with Zn- and Al-forms. The highest conversions of ferrocene over mesoporous molecular sieves (Al)MCM-41 and (Al)SBA-15 were reached over Zn- and H-forms. It was found that Al-forms of mesoporous molecular sieves were not so active in ferrocene acylation compared with the activity of these forms prepared from zeolites Beta and USY. The lowest conversions were obtained with Fe-forms of all the molecular sieves used. The correlation between concentration of Lewis acid sites and ferrocene conversion was found.

In acylation of toluene, Al-forms of zeolites as well as mesoporous catalysts were the most active. The lowest activity in toluene acylation was found for Fe- and H-forms of the molecular sieves used. The selectivities to isopropyl *p*-tolyl ketone at the conversion 20% over zeolite Beta, USY and their ion-exchanged forms with the exception of Fe-forms were higher than 80%. The highest selectivity (more than 95%) to *para*-isomer was obtained with H- and La-forms of both zeolites Beta and USY and also with Al-form of zeolite Beta. The selectivities over mesoporous molecular sieves

(Al)MCM-41 and (Al)SBA-15 and their ion-exchanged forms were lower compared with zeolites. This was due to larger channel diameters of these materials, which enables the formation of sterically more demanding *ortho*-isomer and also consecutive acylation of toluene to diisobutyryltoluenes.

The authors thank the Grant Agency of the Czech Republic (Grants No. 104/07/0383 and No. 203/03/H140) for financial support.

REFERENCES

1. Sen S. E., Smith S. M., Sullivan K. A.: *Tetrahedron* **1999**, *55*, 12657.
2. Čejka J., Wichterlová B.: *Catal. Rev.-Sci. Eng.* **2002**, *44*, 375.
3. De Vos D. E., Jacobs P. A.: *Microporous Mesoporous Mater.* **2005**, *82*, 293.
4. Jana S. K.: *Catal. Surv. Asia* **2006**, *10*, 98.
5. Corma A.: *Chem. Rev.* **1995**, *95*, 559.
6. Červený L., Mikulcová K., Čejka J.: *Appl. Catal., A* **2002**, *223*, 65.
7. Bezouhanova C. P.: *Appl. Catal., A* **2002**, *229*, 127.
8. Klisáková J., Červený L., Čejka J.: *Appl. Catal., A* **2004**, *272*, 79.
9. Casagrande M., Storaro L., Lenarda M., Ganzerla R.: *Appl. Catal., A* **2000**, *201*, 263.
10. Botella P., Corma A., Navarro M. T., Rey F., Sastre G.: *J. Catal.* **2003**, *217*, 406.
11. Neves I., Jayat F., Magnoux P., Perot G., Ribeiro F. R., Gubelmann M., Guisnet M.: *J. Mol. Catal.* **1994**, *93*, 169.
12. Pedro C. L., Apesteguía C. R.: *Catal. Today* **2005**, *107–108*, 258.
13. Freese U., Heinrich F., Roessner F.: *Catal. Today* **1999**, *49*, 237.
14. Beers A. E. W., van Bokhoven J. A., de Lathouder K. M., Kapteijn F., Moulijn J. A.: *J. Catal.* **2003**, *218*, 239.
15. Guignard C., Pedron V., Richard F., Jacquot R., Spagnol M., Coustard J. M., Perot G.: *Appl. Catal., A* **2002**, *234*, 79.
16. Moreau P., Finiels A., Meric P.: *J. Mol. Catal. A* **2000**, *154*, 185.
17. Andy P., Garcia-Martinez J., Lee G., Gonzalez H., Jones C. W., Davis M. E.: *J. Catal.* **2000**, *192*, 215.
18. Hu R. J., Li B. G.: *Catal. Lett.* **2004**, *98*, 43.
19. Zhao D., Huo Q., Feng J., Chmelka B. F., Stucky G. D.: *J. Am. Chem. Soc.* **1998**, *120*, 6024.
20. Mokaya R.: *Chem. Commun.* **2000**, 1891.
21. Wichterlová B., Tvarůžková Z., Sobalík Z., Sarv P.: *Microporous Mesoporous Mater.* **1998**, *24*, 223.
22. Emeis C. A.: *J. Catal.* **1993**, *141*, 347.
23. Dědeček J., Žilková N., Čejka J.: *Microporous Mesoporous Mater.* **2001**, *44*, 259.
24. Wichterlová B., Čejka J.: *Catal. Lett.* **1992**, *16*, 421.